5th International Conference on Experimental Fluid Mechanics – ICEFM 2018 Munich
Munich, Germany, July 2-4, 2018

Time resolved PIV visualization of the generation of coherent structures and their effect on the transition process in narrow rectangular channels

Laurentiu Moruz[1]*, Jens Kitzhofer[1], David Hess[2] and Mircea Dinulescu[1]

[1]Apex Research B.V., Westeinde 10, 2275AD Voorburg, the Netherlands

[2]Dantec Dynamics A/S, Tonsbakken 16-18, 2740 Skovlunde, Denmark

* laurentiu.moruz@apexgroup.eu

Abstract

This work is aiming at extending the understanding of the transition process from a laminar to a turbulent flow field in narrow rectangular channels in isothermal conditions. The role of the upstream inlet geometry and its impact on flow development has been studied. Three inlet geometries have been used to influence the transition process, each geometry having different critical Reynolds number at which the flow is becoming turbulent. The geometries are named square-edged, bell-mouth and undulated geometry. A time resolved Particle Image Velocimetry (PIV) measurement system has been applied in the entrance region for the visualization of coherent vortex structures in terms of vorticity generated by these inlet geometries.

Nomenclature

Re	Reynolds number $\rho \times u_{mean} \times D_{eq}/\mu$ [-]
$Re_{crit,lower}$	lower critical Reynolds number [-]
$Re_{crit,upper}$	upper critical Reynolds number [-]
ρ	density fluid (air) [kg/m^3]
u_{mean}	temporal and spatial average velocity [m/s]
D_{eq}	equivalent diameter 2×h [m]
h	channel gap [m]
w	channel width [m]
μ	dynamic viscosity [Pa s]

1 Introduction

The control of the transition process from a laminar to a turbulent flow field in narrow rectangular channels with flat surfaces has a great importance in Plate-type Heat Exchanger industry, where the requirements for increasing the efficiency is mandatory. This paper is meant to be a modest continuation of the monumental work of Osbourne Reynolds by using the fabulous flow visualization techniques, which now are at our disposal. A large amount of literature describes the characteristics of rectangular channels (internal channel flow) with respect to Reynolds number, friction factor, aspect ratio and surface topology. Nevertheless, most studies describe the laminar or the fully developed turbulent flow field. As stated by Meyer and Olivier, who studied the transition process in round pipes, the transition process is strongly dependent on the inlet geometry. Furthermore, Meyer stated that there is a lack of information in literature with respect to

rectangular channel flows. The difficulty in generating a fully developed turbulent flow field in narrow rectangular channels is already described by Durst et al., who applied Laser Doppler Anemometry in a rectangular water tunnel and identified the need for triggering turbulence to generate a fully developed turbulent velocity profile at low Reynolds numbers. He suggests a vigorous triggering action at the inlet into the channel. The authors of these papers mainly identified the inlet geometry as having major influence on the transition process, which the authors describe in form of Moody Chart. Figure 1 shows the Moody chart generated by differential static pressure measurements in a narrow rectangular channel with 10 mm channel gap and 200 mm width (Set-up 1). The static pressure was measured at locations between $50\times D_{eq}$ and $80\times D_{eq}$ for the three different inlet geometries. Following the observation of Reynolds "…there were two critical values for the velocity in the tubes, the one at which steady motion changes into eddies, the other at which eddies change into steady motion." (p.957), we define a lower and upper critical Reynolds number as shown in figure 1. The bell-mouth geometry has the latest transitional Reynolds numbers, $Re_{crit,lower}$=4000 and $Re_{crit,upper}$=5200 followed by the square-edged geometry with $Re_{crit,lower}$=3800 and $Re_{crit,\ upper}$=4400 and by the undulated geometry with $Re_{crit,lower}$=3200 and $Re_{crit,\ upper}$=4000.

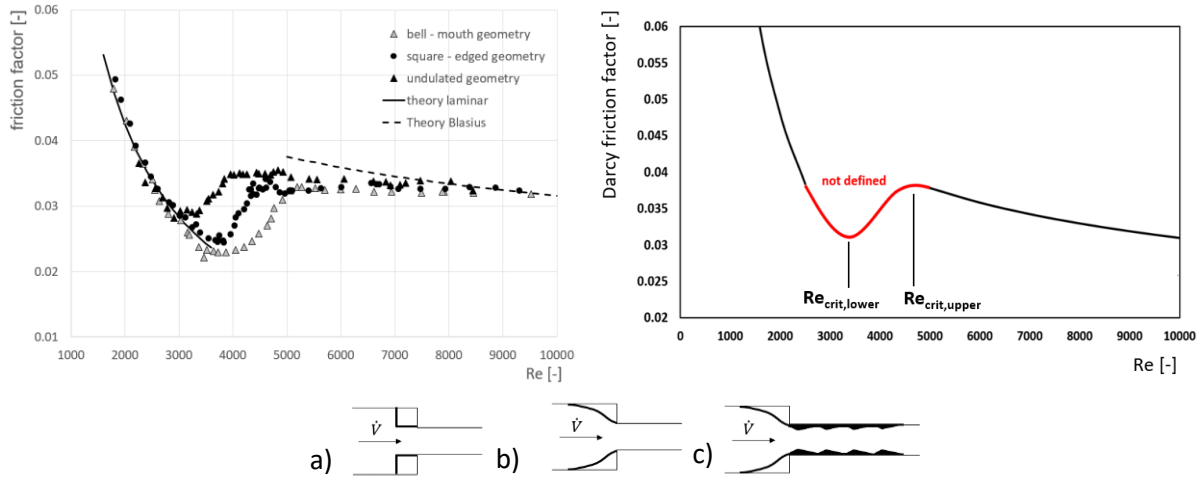

Figure 1: Experimental friction factor diagram as a function of Reynolds number: a) square-edged geometry; b) bell-mouth geometry; c) undulated geometry, theory laminar: 85/Re, theory Blasius: $0.316\times Re^{-0.25}$

Motivated from the results in figure 1, a second scaled-up model has been used for providing a sufficiently high spatial resolution for time resolved Particle Image Velocimetry measurements. This model (Set-up 2) allowed the study of vortical structures at the entrance region of the rectangular channel flow and their influence on the transition process.

2 Experimental Set-up

Figure 2 shows details of the second experimental test facility and of the PIV measurement section. The test rig is made of transparent smooth plexiglass and is composed of a centrifugal fan, a diffuser duct, a settling chamber, an inlet duct and a rectangular channel. Air at room temperature (20°C) is transported by the centrifugal fan through all the facility and is exhausted into the ambient. The centrifugal fan is installed upstream of the flow and has a 4kW electric engine with a maximum flow rate of 6000 m³/h. The volume flow rate is measured with a flow velocity probe from Testo installed at the aspiration side of the fan. To control the airflow rate a variable frequency power supply is used. The diffuser duct is installed at the exit of the centrifugal fan, its purpose being to create a smooth connection to the settling camber without air

flow separation. The settling chamber has a length of 1.75 m and cross section of 0.3×0.3 m with one side being connected to a small confuser-diffuser duct. Two perforated plates with 60% void fraction are installed downstream and upstream of the settling chamber for a uniform flow distribution. Upstream of the contraction and the PIV measurement section a 2.4 m long duct with a cross section 0.125×1 m is installed to generate a quasi developed velocity profile at the inlet of the contraction. The PIV measurement is performed immediately downstream of the contraction having an aspect ratio of 2.5:1 between inlet duct/ rectangular channel. The 50 mm height of the channel is kept constant by attaching on top plate steel U profiles arranged perpendicular to stream flow direction. Insertion of the DHES particles with 1µm size into the air flow rate was done upstream of the centrifugal fan for a homogeneous particle distribution at the PIV measurement position.

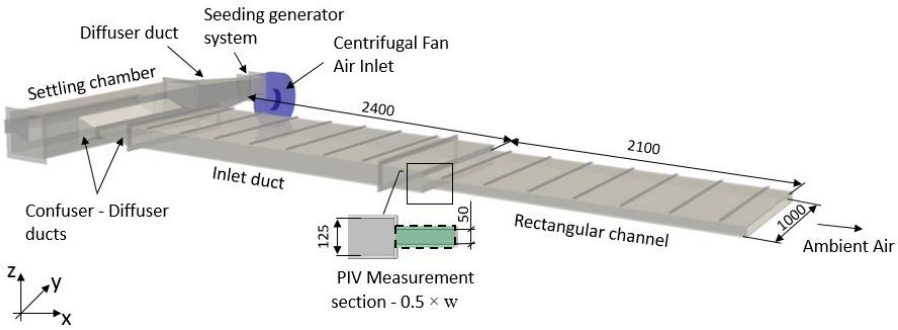

Figure **2**: Model of experimental set-up and PIV measurement section detail with dimensions in millimeters

The seeding particles are illuminated in the xz-plane at y=0.5×w with a 30 mJ dual cavity laser equipped with a Dantec Dynamics light sheet optic. The scattered light of the particles is captured by Dantec Dynamic's 4MP high-speed camera SpeedSense 340 with a maximum of 810 frames per second at full resolution. By cutting the active image area to a rectangular shape (reduction of optical resolution), the maximum temporal resolution was increased to 2000 fps to cover a Reynolds number range of up to 10000. The frame rate was chosen to have a maximum particle displacement of 7 pixel. The observed plane typically has a length of 5 times the channel height and starts right after the inlet, which could be a square-edged, a bell-mouth or an undulated geometry. The number of recorded images was set to 2500 for each Reynolds number and each geometry.

3 Data Reduction

The analysis of the particle images is performed in Dynamic Studio 5.1 with the "Adaptive PIV" routine and wall windowing function to reduce uncertainties due to large shear stress close to the wall. The Cross Correlation algorithm automatically chooses an interrogation area size with respect to number of particles. The minimum number of particles are chosen to be 6/interrogation area. To increase the accuracy in case of large velocity gradients, the algorithm iteratively deforms the interrogation area with respect to shear, rotation and scale. Erroneous vectors are detected by the universal outlier detection method. The scaling is 0.11 mm/Pix. The resulting vector field has a vector pitch of 16 Pix (0.6 vectors/mm). The resulting instantaneous velocity field post-processed by vorticity calculation as well as by a temporal mean. For temporally smoothing the vorticity field, a temporal moving averaging is applied with a basis of 3 vorticity fields. The boundary layer thickness δ_{99} is extracted from the mean vector statistics for each position x downstream of the contraction.

4 Experimental Results

Figure 3 shows the normalized velocity profiles at three different streamwise positions (x/h=1, x/h=2.5, x/h=4) for the three inlet geometries at Re=5150. At the position x/h=1, the square-edged inlet geometry shows a recirculation zone on the top and the bottom wall (vena contracta), while both of the other

geometries only indicate positive velocities. While the velocity profile of the undulated inlet shows a rather top hat velocity profile (which is typical for turbulent flows), the velocity profile of the bell-mouth inlet indicates a more parabolic profile (typical for laminar flows). With further travelling distance, the normalized velocity profiles start to overlap.

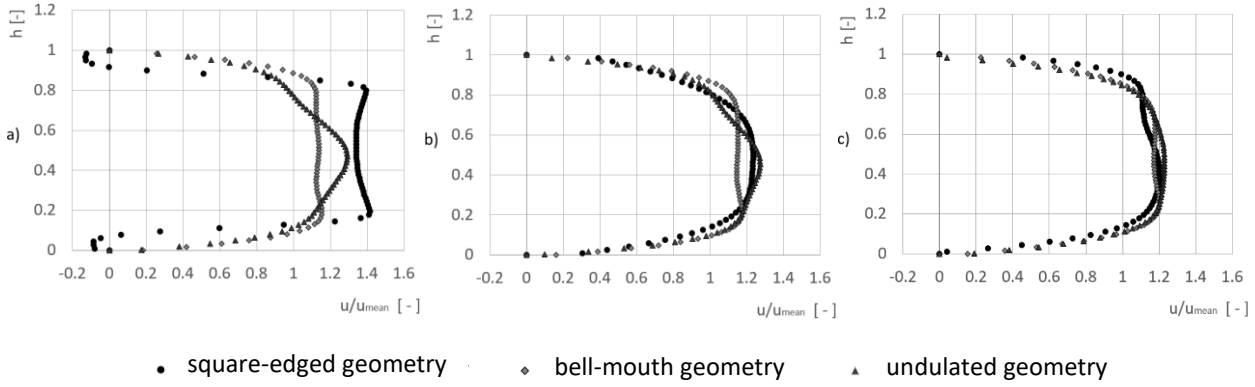

Figure **3**: Normalized mean velocity field characteristics at a) x/h=1, b) x/h=2.5, c) x/h=4

Figure 4 illustrates the boundary layer thickness concept for the entrance region of a channel flow. A boundary layer is formed on the top and on the bottom wall. After a certain entrance length, both boundary layers collide. Thus, the graphs in figure 4 show the distance in between the boundary layers on the one hand as a function of streamwise distance for Re=3400 and on the other hand as a function of Reynolds number at x/h=4. At Re=3400, the distance between the boundary layers is decreasing with a constant gradient for the bell-mouth inlet. For the square-edged inlet geometry, the distance between the boundary layers is rapidly decreasing up to x/h=1 and then slightly decreasing up the x/h=5. The undulated inlet breaks up the boundary layer development showing a constant low distance in between the top and bottom boundary layer over the whole inlet region. At x/h=4, the distance between top and bottom boundary layer grows in the bellmouth case for increasing Reynolds number up to 8000, while the distance decreases for the square-edged geometry and is nearly constant over the whole Reynolds range for the undulated inlet geometry.

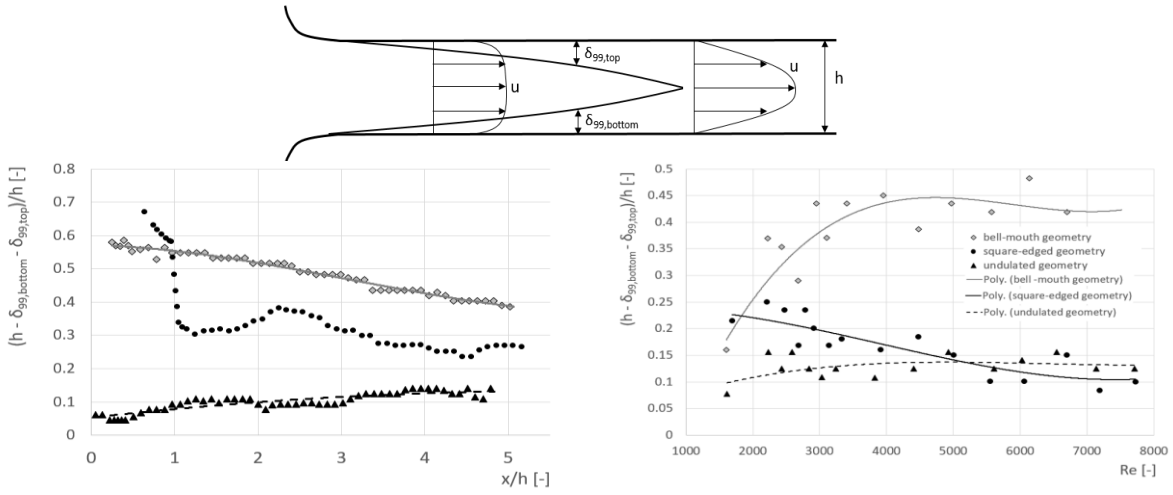

Figure **4**: Boundary layer thickness δ_{99} concept (top), distance in between top and bottom boundary layer as a function of stream wise distance for Re=3400 (bottom left), distance in between top and bottom boundary layer as a function of Reynolds at x/h=4 (bottom right)

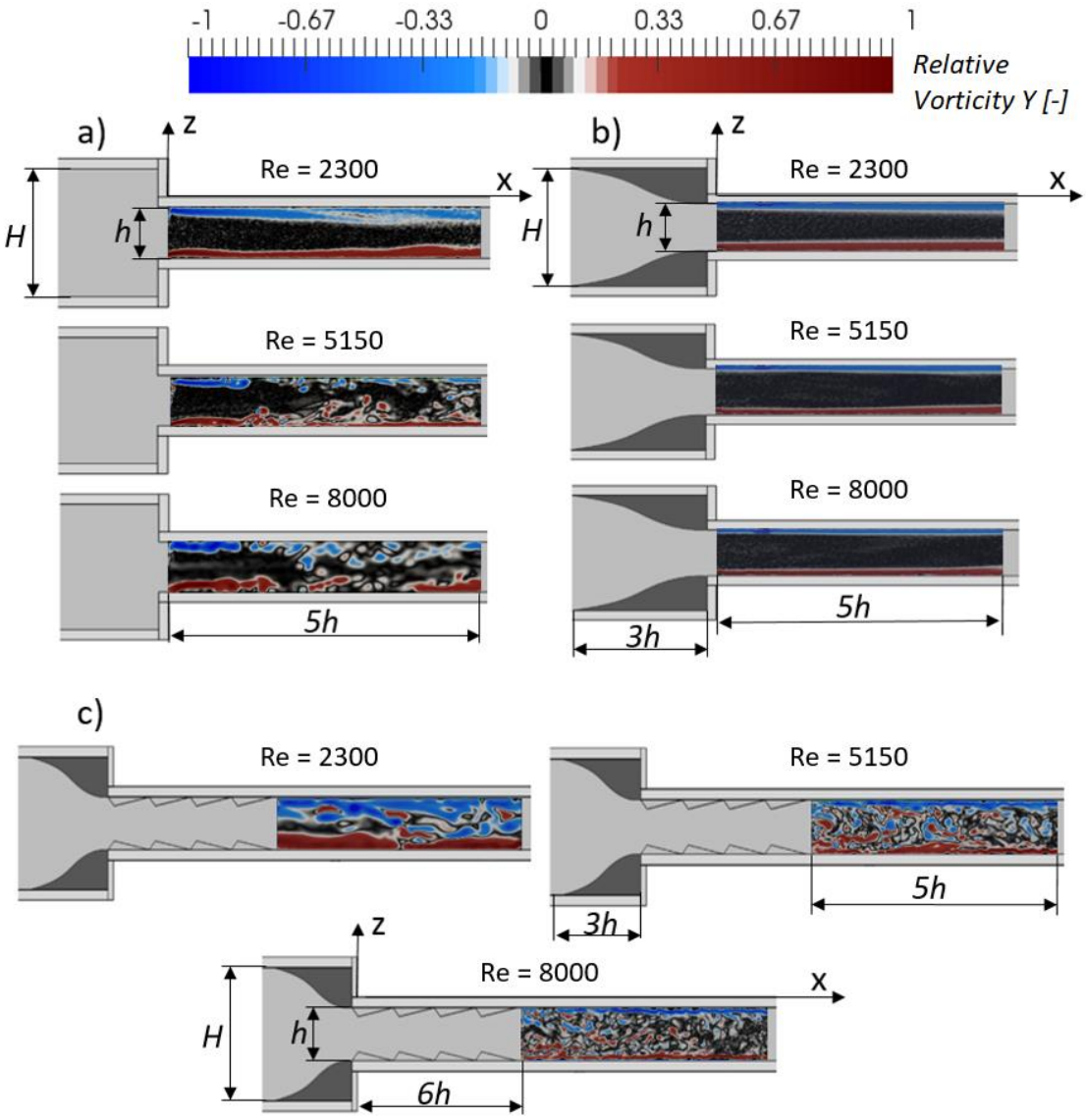

Figure **5**: Instantaneous normalized mean vorticity field characteristics for the different inlet geometries and a low, medium and large Reynolds number of the investigated Reynolds number range

Figure 5 shows the instantaneous relative vorticity fields for different Reynolds numbers and the different inlet geometries (the time resolved vorticity videos will be shown in the presentation and can be downloaded via www.apexgroup.eu). The vorticity is scaled with the maximum vorticity. Blue indicates a counter clockwise rotation and red indicated a clockwise rotation. In case of the bell-mouth inlet geometry, the vorticity stays attached to the wall over the whole investigated Reynolds range. No normalized vorticity is transported into the center of the channel. In case of the square-edged geometry, at low Reynolds numbers the vorticity stays attached to the surface and no vorticity is transported in the center of the channel. As soon as the lower critical Reynolds number is reached, the flow separates at the edge of the contraction and reattaches further downstream generating a recirculation zone. The generated vortices are transported downstream and into the center of the channel, where vortices from top and bottom wall start to interact with each other. At larger Reynolds number, the frequency of the vortex shedding is increased, resulting in

more interactions between top and bottom wall. In case of the undulated geometry, the vorticity layer on top and bottom is not smooth for the lowest Reynolds numbers. Top and bottom vorticity layer are already interacting. For increasing Reynolds numbers, the vortical structures get smaller and occupy the full channel height generating a strong interaction between the top and the bottom wall.

4 Conclusion

There is a clear connection between the friction diagram for the different inlet geometries and the vortical structures generated by the different inlet geometries. While the bell-mouth geometry undergoes a natural transition process, the transition process in case of square-edged geometry and undulated geometry is defined by the perturbations, which generate a forced separation of the boundary layer. In case of the square-edged geometry, separation takes place at the contraction edge forming recirculation zones on top and bottom walls. In case of undulated inlet geometry, the flow exiting the undulated part consists of large vortical structures occupying the whole channel even at low Reynolds numbers. Further post-processing of the data is needed to extract vortex shedding frequencies. Furthermore, future work should focus on more inlet geometries, which may define the transition curve in the friction diagram to generate correlations for the transition region depending on the installed inlet geometry.

Acknowledgements

The authors gratefully acknowledge partially funding received by the Ministry of Economic Affairs and Climate Policy from the Netherlands. Thanks are also due to Kenan Golgyaz for the organization of the time resolved PIV system and the helpful hands during measurements.

References

Reynolds O (1883) An Experimental Investigation of the Circumstances Which Determine Whether the Motion of Water Shall Be Direct or Sinuous, and of the Law of Resistance in Parallel Channels. *Philosophical Transactions of the Royal Society of London* 174:935-982

Reynolds O (1895) On the Dynamical Theory of Incompressible Viscous Fluids and the Determination of the Criterion. *Philosophical Transactions of the Royal Society of London* 186:123-164

Meyer JP and Olivier JA (2011) Transitional flow inside enhanced tubes for fully developed and developing flow with different types of inlet disturbances: Part I–Adiabatic pressure drops. *International Journal of Heat and Mass Transfer* 54.7:1587-1597

Meyer JP (2014) Heat transfer in tubes in the transitional flow regime. In: *Proceedings of the 15th International Heat Transfer Conference, Kyoto, paper* KN03:11-15

Durst F, Fischer M, Jovanovic J, and Kikura H (1998) Methods to set up and investigate low Reynolds number, fully developed turbulent plane channel flows. *Journal of fluids engineering* 120.3:496-503